The Wistar Institute of Anatomy and Biology

Annual Progress Report: 2012 Formula Grant

Reporting Period

July 1, 2013 – June 30, 2014

Formula Grant Overview

The Wistar Institute of Anatomy and Biology received $1,491,186 in formula funds for the grant award period January 1, 2013 through June 30, 2014. Accomplishments for the reporting period are described below.

Research Project 1: Project Title and Purpose

Informatics Solutions for NextGen Sequence Data Analysis – Recent genome-wide studies suggest that at least half of the human genes, including many therapeutic target genes, produce multiple protein isoforms through alternative transcription. Many of the isoforms produced in this manner are tightly regulated during normal development but are mis-regulated in cancer cells. We propose to develop novel algorithms and build an informatics platform for understanding gene regulation at isoform-level (alternative promoter or alternative transcript-level) by developing statistically rigorous bioinformatics resources for processing Next-Generation Sequencing (NGS) data to better understand gene regulatory mechanisms in mammalian cells, and more importantly, how dis-regulation of these mechanisms leads to cancer. The informatics platform will be tested by analyzing The Cancer Genome Atlas data.

Duration of Project

1/1/2013 – 6/30/2014

Project Overview

In recent years, the notion of "one gene makes one protein that functions in one signaling pathway" in mammalian cells has been shown to be overly simplistic. Recent evidence suggests that more than 50% of the human genes produce multiple protein isoforms, through alternative splicing and alternative usage of transcription initiation and/or termination. Notably, the disruption of many of these genes is implicated in cancer and several neuropsychiatric disorders. For majority of human genes the resulting multiple protein isoforms are functionally different and can participate in different signaling pathways. We propose to build an informatics platform for understanding gene regulation at isoform-level by developing statically rigorous bioinformatics resources for processing NGS data. Recently, computational approaches that combine seemingly disparate experimental data have been successful in developing concise gene regulation models and transcriptional modules. We plan to extend these methodologies to perform integrative analysis of multiple high-throughput data sets, such as The Cancer Genome

Atlas (TCGA) datasets. We will apply innovative statistical modeling approaches that combine state-of-the-art meta-classification algorithms, such as Naïve Bayes Tree, Bagging and LogitBoost, with Random Forest feature selection to classify different types of target promoters with good classification accuracy and reduced instability, in order to predict differentially active gene promoters, their transcript variants and infer the protein-DNA interactions from Ribonucleic Acid Sequencing (RNA-seq) and Chromatin Immunoprecipitation Sequencing (ChIP-seq) data. This will be completed by pursuing the following aims, (1) Develop statistically rigorous novel algorithms and bioinformatics pipelines to identify the orthologous promoters, corresponding transcript variants and protein isoforms that are conserved between human and mouse, and (2) develop novel algorithms and informatics pipelines for integrative analysis of NGS datasets to estimate the activity and expression of both known and novel promoters and their transcript variants, in various tissues, developmental stages, and different cancer types by data-mining of The Cancer Genome Atlas data.

Principal Investigator

Ramana V. Davuluri, PhD
Associate Professor
The Wistar Institute
3601 Spruce Street
Philadelphia, PA 19104

Other Participating Researchers

Louise Showe, PhD; Sharmistha Pal, PhD; Yingtao Bi, PhD – employed by The Wistar Institute

Expected Research Outcomes and Benefits

An important question of immediate attention that will be addressed by this project is “which alternative promoters and their transcript variants of human genes are preferentially silenced or activated in cancer cells and different cancer types”. This project will develop novel bioinformatics methods to determine the orthologous human-mouse pairs of primary and alternative promoters, their corresponding transcript variants and the protein isoforms they encode. And, novel algorithms will be developed to estimate the activity of alternative promoters and alternative transcripts in different tissues and their developmental stages and cancer types, from integrative analysis of NGS datasets. We will test and validate various statistical machine-learning methods in the development of efficient bioinformatics pipelines. The broad potential impact on the field of biomedical informatics is development of novel algorithms and informatics pipelines for *in silico* discovery and research for accelerating the linkage of phenotypic and genomic information, at gene-isoform level by making use of NGS data. We believe this research will identify a large number of novel targets for the diagnosis and treatment of different cancers. We have earlier discovered the wide-spread use of alternative promoters and splicing in mammalian genes by using the ChIP-seq and RNA-seq approaches in brain development. For example, alternative splicing of Vascular Endothelial Growth Factor A (VEGFA) gene yields multiple proangiogenic, and paradoxically, anti-angiogenic isoforms. Accordingly, for the majority of glioblastoma "driver" genes, the inclusion/exclusion of exonic

sequences generate transcript variants and /or protein isoforms that vary in structure and function. For example, imagine a drug that suppresses expression of a specific form of VEGFA, while sparing the other isoforms that control expression of this gene in healthy tissues. By targeting the specific problematic gene isoform, a more effective treatment with fewer side effects can be administered. It is not hard to imagine how specific targeting of individual gene isoforms could lead to more accurate and sensitive diagnoses as well.

Summary of Research Completed

Studies and Results

Aim 1 – Develop statistically rigorous novel algorithms and bioinformatics pipelines to identify the orthologous promoters, corresponding transcript variants and protein isoforms that are conserved between human and mouse. There are no results to report at this time.

Aim 2 - Develop novel algorithms and informatics pipelines for integrative analysis of NGS datasets to estimate the activity and expression of both known and novel promoters and their transcript variants, in various tissues, developmental stages, and different cancer types by data-mining of The Cancer Genome Atlas data. The results pertaining to Aim 2 are summarized below.

PIGExClass – Platform-independent Isoform-level Gene-Expression based Classification-system
Molecular stratification of tumors is essential for developing personalized therapies. Although patient stratification strategies have been successful; computational methods to accurately translate the gene-signature from high-throughput platform to a clinically adaptable low-dimensional platform are currently lacking. We developed a platform-independent isoform-level gene-expression based classification-system (PIGExClass), a novel computational approach to derive and then transfer isoform-level gene-signatures from one analytical platform to another. We applied PIGExClass to design a reverse transcriptase-quantitative polymerase chain reaction (RT-qPCR) based molecular-subtyping assay for glioblastoma multiforme (GBM), the most aggressive primary brain tumors. Unsupervised clustering of TCGA (the Cancer Genome Atlas Consortium) GBM samples, based on isoform-level gene-expression profiles, recaptured the four known molecular subgroups but switched the subtype for 19% of the samples, resulting in significant ($P = 0.0103$) survival differences among the refined subgroups. PIGExClass derived four-class classifier, which requires only 121 transcript-variants, assigns GBM patients' molecular subtype with 92% accuracy. This classifier was translated to an RT-qPCR assay and validated in an independent cohort of 206 GBM samples. Our results demonstrate the efficacy of PIGExClass in the design of clinically adaptable molecular subtyping assay and have implications for developing robust diagnostic assays for cancer patient stratification.

Evaluation of algorithms for isoform-level expression estimation from RNA-seq data
Both hybridization and sequencing-based approaches have been developed for transcriptome studies. High density exon-array has been successfully used to study alterative splicing events. With the advent of NGS technologies, RNA-seq has also emerged as a powerful tool for transcriptome analysis. The analysis of RNA-seq data is a challenging task. In the last few years, plenty of tools have been developed to estimate the abundance of gene expression at transcript

level. We performed a comparative study between different exon-array and RNA-seq tools using The Cancer Genome Atlas (TCGA) GBM data. We designed RT-qPCR assay as a gold standard to benchmark the gene expression values by RNA-seq and Exon-array. Previous studies indicate strong correlation between gene-level expression estimates from RNA-seq and Exon-array data. However, we found poor correlation between RT-qPCR and Exon-array/RNA-seq for isoform/transcript-level expression estimates and better correlation for fold change values. We found that the transcript-level fold-change estimates (tumor over normal) obtained by Multiple Mapping Bayesian Gene Expression (MMBGX) from exon-array data correlated well with RT-qPCR values. RNA-Seq by Expectation-Maximization (RSEM) outperformed the other algorithms (Table 1).

Short-read based annotation pipeline for mapping and analyzing ChIP-seq data:
Mapping genome-wide data to human subtelomeres has been problematic due to the incomplete assembly and challenges of low-copy repetitive DNA elements. In collaboration with Riethman laboratory at The Wistar Institute, we developed a novel bioinformatics pipeline incorporating multi-read mapping for annotation of the updated assemblies using short-read data sets.

Table 1: Correlation between RT-qPCR based values and isoform-level expression estimates by MMBGX (Exon-array) and RNA-seq algorithms. The Pearson correlation coefficients were computed using 159 transcripts measured by all platforms.

Algorithm	Correlation coefficient based on	
	Expression	Fold-change
Cufflinks (http://cufflinks.cbcb.umd.edu/)	0.156	0.684
RSEM (http://deweylab.biostat.wisc.edu/rsem/)	0.338	0.743
eXpress (http://bio.math.berkeley.edu/eXpress/index.html)	0.321	0.587
IsoformEx (http://bioinformatics.wistar.upenn.edu/isoformex)	0.286	0.660
MMBGX (Exon-array) http://www.bgx.org.uk/software/mmbgx.html	0.43	0.825

Research Project 2: Project Title and Purpose

Regulation of Immune Responses in Multiple Myeloma Bone Marrow Microenvironment – The purpose of this project is to evaluate the contribution of bone marrow immature myeloid cells in insufficient immune responses observed in multiple myeloma and validate strategy aimed to improve anti-tumor immune responses based on targeting these cells.

Duration of Project

1/1/2013 – 6/30/2014

Project Overview

The goal of this project is to understand the function of bone marrow immature myeloid cells in multiple myeloma (MM), a blood cancer characterized by uncontrolled growth of malignant plasma cells preferentially in the bone marrow. Using *in vivo* immunocompetent mouse model of MM we will investigate whether immature myeloid cells expand and accumulate in this disease. We will also evaluate whether these cells are functionally changed in MM. Specifically, the ability of immature myeloid cells to suppress immune responses and thus, become so-called myeloid derived suppressor cells (MDSC), will be determined. Our study will also provide an insight into the kinetic of antigen-specific immune response in MM and investigate the mechanisms by which MDSC could regulate function of immune cells in the bone marrow. Finally, we will determine whether targeting of MDSC could improve anti-tumor immune responses leading to decreased MM burden. The following Specific Aims will be addressed: (1) investigate the involvement of MDSC in regulation of immune responses in MM BM; and (2) determine whether targeting MDSC would improve the anti-tumor immune response in MM. The knowledge gained from this project will be important as it may justify a novel therapeutic approach for treatment of multiple myeloma based on targeting MDSC.

Principal Investigator

Yulia Nefedova, MD, PhD
Assistant Professor
The Wistar Institute of Anatomy and Biology
3601 Spruce Street
Philadelphia, PA 19104

Other Participating Researchers

None

Expected Research Outcomes and Benefits

This project will address the following questions: Do immature myeloid cells expand in the bone marrow during multiple myeloma progression? Do they acquire an ability to suppress immune responses? What is the mechanism(s) responsible for immunosuppressive activity of immature myeloid cells in multiple myeloma? Is there an antigen-specific T cell response generated in the bone marrow in multiple myeloma and what is the contribution of immature myeloid cells in this immune response? Would targeting immature myeloid cells improve anti-tumor immune responses and decrease tumor burden in multiple myeloma? The answers to these questions will lead to a better understanding the function of immature myeloid cells and the mechanisms of immune suppression in the bone marrow in multiple myeloma. This information will not only provide us with a greater understanding of the immunobiology of this disease, but also may validate a novel therapeutic approach based on targeting immature myeloid cells in multiple myeloma as well as the factors or signaling pathways that mediate the immunosuppressive effect of these cells. If successful, targeting of immature myeloid cells in multiple myeloma would ultimately result in improved anti-tumor immunity and delayed disease

progression.

Summary of Research Completed

Specific Aim 1

We evaluated the presence of different populations of myeloid-derived suppressor cells (MDSC) in bone marrow (BM) and peripheral blood (PB) of newly diagnosed, non-treated patients with multiple myeloma (MM). These populations included: MDSC - $CD11b^{+}CD14^{-}CD33^{+}$; PMN-MDSC - $CD11b^{+}CD14^{-}CD33^{+}CD15^{+}$; and M-MDSC - $CD11b^{+}CD14^{-}CD33^{+}CD15^{-}$. Cells with the same phenotypes in control donors were called immature myeloid cells (IMC). Since MM cells constitute a significant proportion of MM BM, the frequency of MDSC was evaluated as the proportion of these cells among the $CD138^{-}$ non-myeloma cells of BM. Mononuclear cells were isolated by Ficoll-Paque density gradient centrifugation, labeled with corresponding antibodies and subjected to flow cytometry using the LSR II instrument (BD Biosciences). Our data demonstrated a significant ($p<0.05$) accumulation of MDSC in BM of MM patients, as compared to healthy donors (Fig. 1A). MDSC represented 41.1±5.3% (range from 13.3% to 75.9%) of BM cells in MM, while IMC with the same phenotype represented only 22.9±2.8% (range from 7.7% to 33.3%). A significant accumulation of MDSC was also observed in PB of MM patients (Fig. 1A). Polymorphonuclear MDSC (PMN-MDSC) represented the majority of MDSC in BM and was significantly increased in BM and PB of MM patients, as compared to healthy donors (Fig. 1B). In contrast, no differences in the proportions of $CD11b^{+}CD14^{-}CD33^{+}CD15^{-}$ M-MDSC were found (Fig. 1C). This was consistent with the lack of differences in the presence of $CD11b^{+}CD14^{+}HLA\text{-}DR^{-}/^{low}$ cells (data not shown), which are considered to be a distinct population of monocytic MDSC (M-MDSC).

To verify whether the population of cells with the phenotype of MDSC that accumulates in BM of MM patients, could be functionally defined as MDSC, we determined their immune suppressive activity. Populations of MDSC or IMC were isolated by flow sorting using the FASCAria instrument (BD Biosciences). Human T cells were purified from PB mononuclear cells (PBMC) obtained from healthy donors, using T cell enrichment columns (R&D Systems). Dendritic cells were generated *in vitro* from PBMC obtained from a different donor. T cells ($1x10^{5}$) were stimulated with lipopolysaccharide -matured dendritic cells ($1.5x10^{4}$), with or without MDSC present in the co-culture. The number of interferon (IFN)-γ-producing T cells was evaluated in an enzyme-linked immunospot (ELISPOT) assay on automatic counter (Cellular Technology). Proliferation of T cells was measured by ^{3}H-Thymidine incorporation. IMC isolated from BM of healthy donors were used as control. A significant inhibition of T cell activity by MDSC was observed (Fig. 2A,C), whereas IMC lacked suppressive activity (Fig. 2B,D). These data indicate that MDSC with immune suppressive activity accumulated in BM of MM patients. We evaluated an expression of several genes previously implicated in MDSC-mediated immune suppression. Gene expression of arginase-1, Cybb and Cox-2 was significantly up-regulated in MDSC isolated from BM of MM patients as compared to IMC isolated from BM of healthy donors (data not shown). There was no difference in reactive oxygen species (ROS) and inducible nitric oxide synthase (iNOS) levels between MDSC and IMC (data not shown).

Specific Aim 2

To address a possible role of MDSC in MM, we used S100A9KO mice ENFREF 17. Under physiological conditions, these mice demonstrated normal myeloid cell differentiation. However, when challenged with tumor cells, S100A9KO mice showed a reduced accumulation of MDSC as compared to their wild-type (WT) counterparts. Consistent with previously reported data, no differences were found in the presence of IMC in the spleens and lymph nodes (data not shown) between WT and S100A9KO tumor-free mice. However, in BM of S100A9KO mice, the presence of IMC was significantly reduced. To evaluate the effect of S100A9 deficiency on MM growth and mice survival from MM, BCM and DP42 tumors were established in WT or S100A9KO mice. No difference in BM tumor burden was observed between WT and S100A9KO mice during MM progression. Although S100A9KO BCM-bearing mice demonstrated a slight survival advantage as compared to WT mice, the difference was not statistically significant. In DP42-bearing mice, no evidence of improved survival was observed.

These data raised the question as to what role, if any, MDSC could play in MM progression in BM. One of the major effects of MDSC is the inhibition of antigen-specific immune responses. Rapid growth of MM in BCM and DP42 models, 100% tumor take, and the lack of spontaneous rejection suggested that these tumor cells are likely to be poorly immunogeneic. To investigate the effect of MDSC in the model of a more immunogeneic tumor, we generated a DP42 cell line with a stable overexpression of ovalbumin (OVA): DP42-OVA. DP42-OVA cells had similar kinetics of growth *in vitro* as compared to parental DP42 cells. However, S100A9KO mice, inoculated with DP42-OVA cells, demonstrated significantly improved survival ($p=0.009$) and delayed tumor growth in BM, as compared to WT mice. We compared the presence of Gr-1^+CD11b$^+$ MDSC in BM of WT and S100A9 mice one week after MM inoculation. At this point, the number of tumor cells in BM and spleens of both groups of mice was the same. MDSC in BM of DP42-OVA-bearing WT mice was increased, as compared to tumor-free mice. The presence of MDSC in BM of DP42-OVA-bearing S100A9KO mice was significantly ($p=0.04$) lower. MDSC isolated from BM of DP42-OVA-bearing WT mice one week after tumor inoculation suppressed antigen-specific T cell response, whereas MDSC from S100A9KO MM-bearing mice lacked this ability. These results suggest that the loss of immune suppressive activity in S100A9KO mice was likely the result of a decreased proportion of immune suppressive MDSC among BM Gr-1^+CD11b$^+$ cells.

To investigate the involvement of the immune mechanisms in decreased tumor growth of MM in S100A9KO mice, we depleted CD8$^+$ T cells using CD8 monoclonal antibody (Ab, Clone: 53-6.72, BioXCell, West Lebanon, NH). Mice were treated i.p. with 200µg of CD8 antibody or control IgG2b (clone LTF-2, BioXCell) every 4 days, beginning 4 days after tumor cell injection (total of 6 injections of anti-CD8 Ab or control IgG). Administration of this antibody completely abrogated the improved survival of S100A9KO mice inoculated with DP42-OVA MM cells (Fig. 3A). To investigate whether the decreased presence of MDSC in MM-bearing S100A9KO mice would result in an improved tumor-specific immune response, we measured the presence of OVA-specific CD8$^+$ T cells in DP42-OVA-bearing mice, using SIINFEIKL-H2K^b pentamers. After one week, S100A9KO mice had a higher presence of pentamer-positive CD8$^+$ T cells in BM; however, the difference was not statistically significant. But by week three, the presence of pentamer-positive CD8$^+$ T cells was significantly higher in BM of DP42-OVA-bearing

S100A9KO than in WT mice (Fig. 3B). Similar kinetics were observed in spleens of these mice (Fig. 3C). However, at all time points the proportion of pentamer-positive $CD8^+$ T cells in spleens was more than 10-fold lower than in BM (Fig. 3D,E) indicating that BM was the primary site of accumulation of antigen-specific $CD8^+$ T cells in S100A9KO MM-bearing mice.

We also evaluated the presence of IFN-γ^+ (Th1-type) $CD4^+$ T cells in MM-bearing mice. A slight increase in the proportion of these cells was observed one week after tumor inoculation in BM of S100A9KO mice. A week later the differences became significant (Fig. 3D). There was no increase in the proportion of IFN-γ positive cells in spleens (Fig. 3E). To confirm the contribution of MDSC in MM tumor growth an adoptive transfer of $Gr1^+CD11b^+$ cells isolated from BM of WT DP42-bearing mice was performed into recipient S100A9KO DP42-OVA bearing mice. $Gr1^+CD11b^+$ MDSC were isolated from BM of DP42-bearing mice by flow sorting 10 days after tumor cell inoculation. MDSC (5×10^6) were injected i.v. into the tail vein of DP42-OVA bearing mice every 4 days, beginning on day 4 after DP42-OVA tumor cell injection. The mice received a total of 4 injections of MDSC. The transfer of WT MDSC into MM-bearing S100A9KO mice resulted in a significantly decreased survival of these mice (Fig. 3F).

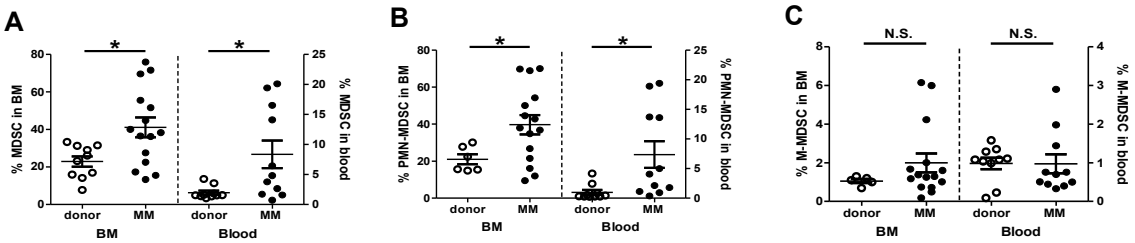

Figure 1. *Accumulation of MDSC in patients with MM*. BM and PB samples were obtained from patients with MM (n=15 and n=11, respectively) or healthy donors (n=6 and n=10, respectively). Mononuclear cells were labeled with specified antibodies and analyzed by flow cytometry. Proportion of the following cell populations was evaluated: (**A**) $CD11b^+CD14^-CD33^+$ MDSC, (**B**) $CD11b^+CD14^-CD33^+CD15^+$ PMN-MDSC, and (**C**) $CD11b^+CD14^-CD33^+CD15^-$ M-MDSC. Presented data show proportions of these cells calculated among $CD138^-$ non-myeloma cell.
* - Statistical significance between groups ($p<0.05$).

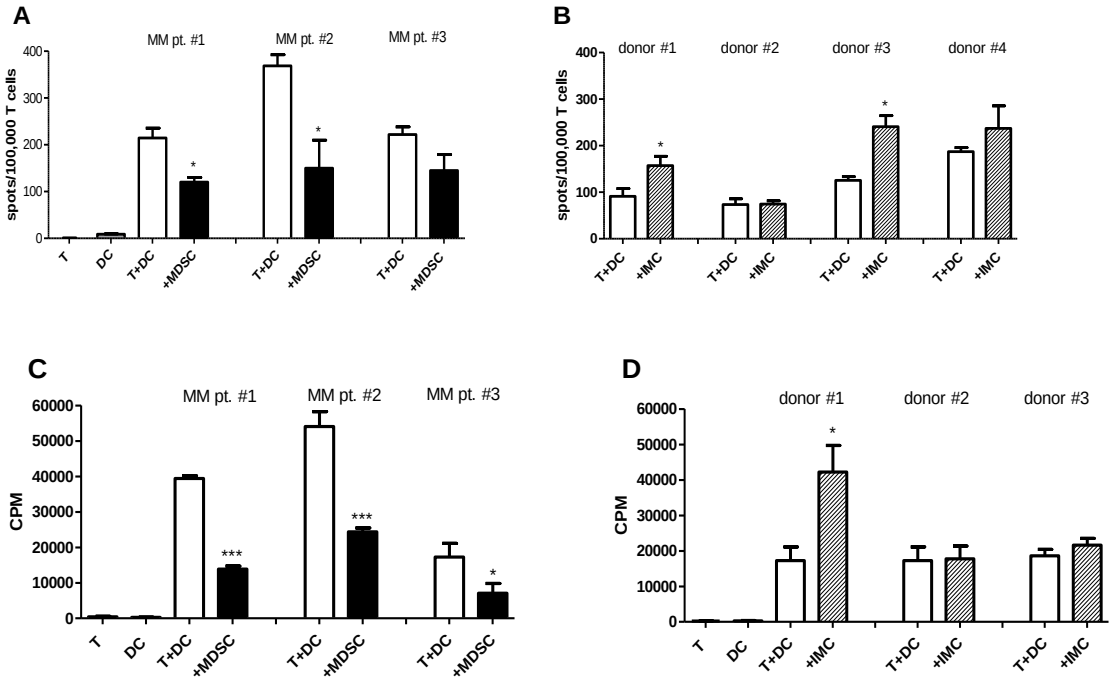

Figure 2. *Suppressive activity of MDSC isolated from patients with MM*. $CD11b^{+}CD14^{-}CD33^{+}$ cells were isolated by sorting of BM from MM patients (**A,C**) or healthy donors (**B,D**). Sorted cells were added at 1:1 ratio to purified T cells stimulated by allogeneic dendritic cells. (**A,B**) The secretion of IFN-γ was measured by ELISPOT after 48 hours of incubation. (**C-D**) T cell proliferation was measured by ^{3}H-Thymidine incorporation. Each condition was set up in triplicate. Statistically significant differences between samples with and without MDSC:
* - $p<0.05$; *** - $p<0.005$.

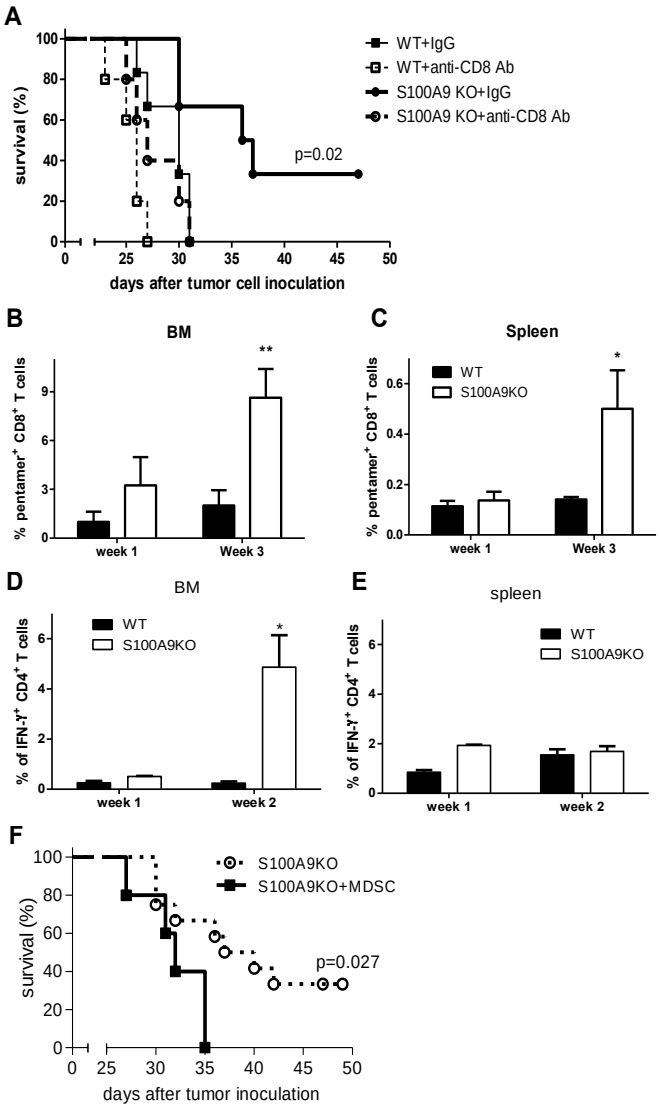

Figure 3. *Tumor-specific T cell responses in MM*. DP42-OVA tumors were established in S100A9KO or WT mice. (**A**) Four days after tumor cell inoculation each group was split into two and treatment with anti-CD8 antibody or control IgG was initiated. Mice survival was evaluated. (**C-D**) DP42-OVA bearing mice were euthanized at indicated time points. BM and spleens were collected and labeled with anti-CD8 antibody and SIINFEKL-H2-K^b pentamer conjugated with FITC and analyzed by flow cytometry. (**B**) Proportion of ova-specific $CD8^+$ T cells in BM and spleens (**C**) * - statistical significance $p<0.05$; ** - statistical significance $p<0.01$ between S100A9KO and WT group of mice. BM (**D**) and spleens (**E**) were collected from DP42-OVA bearing S100A9KO and WT mice. Proportion of IFN-γ^+CD4^+ T cells was determined by flow cytometry. Three mice per group were analyzed. All experiments were repeated twice. * - indicate significant difference $p<0.05$. (**F**) MDSC were isolated from DP42-bearing WT mice and $5x10^6$ cells were injected i.v. into DP42-OVA-bearing S100A9KO mice on days 4, 8, 12 and 16 after tumor cell inoculation. Survival of DP42-OVA bearing S100A9KO mice with (n=5) or without (n=12) transferred MDSC was determined.

Research Project 3: Project Title and Purpose

Molecular Basis of BRCA1 and PALB2 Tumor Suppression – Our long-term goal is to detail the molecular basis of tumor suppressor activity of the breast and ovarian cancer susceptibility genes Breast Cancer 1 (BRCA1) and Partner and Localizer of Breast Cancer 2 (PALB2) in order to develop a more rational and effective therapy following inactivation of these genes in breast and ovarian cancers. We postulate that BRCA1 and PALB2 are transducers of multiple signaling pathways and their functional inactivation in breast and ovarian epithelial cells lead to a loss of responsiveness to extracellular signals. Our working hypothesis is that the tumor suppressor activity of BRCA1 and PALB2 is due to their function as co-activators of transcription for growth inhibitory signals.

Duration of Project

1/1/2013 – 6/30/2014

Project Overview

We postulate that breast and ovarian cancer susceptibility genes (BRCA1 and PALB2) are transducers of multiple signaling pathways and their functional inactivation in breast and ovarian epithelial cells lead to a loss of responsiveness to extracellular signals. We envision that the breast and ovarian cancer susceptibility genes function in transcriptional regulation to mediate mammary epithelial cell morphogenesis and differentiation. Our working hypothesis is that the tumor suppressor activity of BRCA1 and PALB2 is due to their function as co-activators of transcription for growth inhibitory signals.

Specific Aims:
1: Determine the molecular basis by which BRCA1 and PALB2 activate transcription in response to NF-kB and RA.
2: Determine how cancer-causing mutations in BRCA1 alter their function at its target genes.

Our studies pinpoint a key role for BRCA1 and PALB2 in transcriptional responsiveness to nuclear factor kappa-light-chain-enhancer of activated B cells (NF-kB) and retinoic acid (RA), an inhibitory signal, in non-transformed breast epithelial cells. In this project, we will assess the mechanism by which BRCA1 and PALB2 mediate activation of NF-kB and retinoic acid responsive genes and dissect the critical domains in BRCA1 and PALB2 required for their function. Our focus will be to understand the functional domains in BRCA1 and PALB2 that are required for transcriptional activation and to dissect the molecular basis for the requirement of such domains. This is particularly critical for the BRCA1 C Terminus (BRCT) domain as it may reveal the molecular basis of BRCA1 tumor suppressor activity. All these experiments will be performed using a panel of breast and ovarian cancer cell lines as to insure the generality of our findings with regards to the molecular mechanism of BRCA1 and PALB2.

Principal Investigator

Ramin Shiekhattar, PhD
Professor
The Wistar Institute
3601 Spruce St
Philadelphia, PA 19104Professor

Other Participating Researchers

Matteo Cesaroni, PhD; Alessandro Gardini, PhD; Neil Cooch; Fan Lai, PhD – employed by The Wistar Institute

Expected Research Outcomes and Benefits

We applied the method of Chromatin Immunoprecipitation Sequencing (ChIP-seq), which was often used in the past for studies of chromatin regulatory complexes to uncover the genomic sites occupied by breast and ovarian cancer genes. This approach had not been tried with breast cancer and fanconi anemia genes and is the unique aspect of our studies. Identification of the genomic sites at which these proteins reside provides a foundation for detailed analysis of their normal function and how their misregulation leads to cellular transformation. Our efforts in combining genomic approaches with functional studies have uncovered a role for these proteins as co-activators of NF-kB and retinoic acid signaling. The application challenges our current thinking regarding the BRCA1 and PALB2 function, by proposing a role for these proteins in regulating activated levels of transcription in response to extracellular signaling important for differentiation and proliferation.

By identifying the exact targets for these cancer genes, we will provide a functional readout (both gene expression changes and possible epigenetic changes) for the assessment of cancer causing mutations in these genes.

Summary of Research Completed

Please note that the following are cell line identifiers and not acronyms: MCF10A, MCF7, HCC1937, HCT116, HeLa

Aim 1: Detailed analysis of BRCA1 and PALB2 in Retinoic Acid function.
To complete our analysis on the transcriptional regulation by Breast Cancer 1 (BRCA1) and Partner and Localizer of Breast Cancer 2 (PALB2), we investigated the response to Retinoic Acid genome-wide in breast cancer cells.

Role of BRCA1 and PALB2 in stimulus-dependent activation.
Our functional analysis of MCF10A and MCF7 cells pointed to a role for BRCA1 and PALB2 in transcriptional activation of Nuclear Factor (NF)-kB responsive genes. Since these proteins occupy a large number of transcriptionally active genes, we envisage that they may play a broader role in stimulus-dependent transcriptional activation. To test this contention, we

examined three well-characterized signaling pathways, implicated in breast cancer: p53, epidermal growth factor (EGF) and Retinoic Acid (RA). Neither activation of the p53 pathway following Nutlin 3 treatment, nor EGF-mediated stimulation of immediate early genes were significantly affected by depletion of BRCA1 or PALB2 (Figure 1A and B).

Role of BRCA1 and PALB2 in Retinoic Acid signaling.

We then turned our attention to the retinoic acid (RA) signaling, which was previously shown to have anti-proliferative effects in breast cancer cells. Strikingly, the RA signaling showed a compelling requirement for BRCA1 and PALB2. Treatment of MCF7 cells with RA led to a concomitant increase in the recruitment of RNA Polymerase II (RNAPII), BRCA1 and PALB2 on Homeobox Protein Hox A1 (HOXA1) and Homeobox Protein Hox A2 (HOXA2) genes supporting a direct function for these breast cancer susceptibility proteins in RA responsiveness (Figure 2A and B). Importantly, BRCA1 and PALB2 are not only recruited at the transcriptional start site (TSS) following stimulation with RA but also accumulate at the 3' end of genes (Figure 2A and B). We next turned to examining the functional impact of BRCA1 and PALB2 on RA responsiveness. While treatment with RA induced a ~50 and ~20 fold activation of HOXA1 and HOXA2 genes, respectively, depletion of PALB2 or BRCA1 reduced the RA-induced activation to 10 fold for each gene (Figure 2C). Importantly, depletion of retinoic acid receptor (RARa) diminished the recruitment of BRCA1, PALB2 and RNAPII following RA treatment concomitant with decreased RA-responsiveness (Figure 2D). These results point to a role for RARa in recruitment of BRCA proteins.

To assess the breadth of action of PALB2 and BRCA1 in RA responsiveness, we treated MCF7 cells with RA and performed a gene expression profiling using microarrays. Importantly, depletion of BRCA1 and PALB2 in three independent experiments blunted the responsiveness of nearly all RA responsive genes (248 genes), underscoring the importance of these proteins in RA signaling (Figure 2E). Besides genes with known roles in RA mediated apoptosis signaling, many genes involved in oxidative stress and interferon signaling lost their responsiveness to RA following depletion of BRCA1 and PALB2 (Figure 2F).

RA acid induces growth suppression in a wide range of adult cells, including breast cancer cells. We tested the hypothesis that depletion of BRCA1 and PALB2, which resulted in impaired transcriptional response to RA, may also diminish the RA-mediated growth suppression using MCF7 cells. Indeed, depletion of BRCA1 or PALB2 resulted in a significant decrease in the RA-mediated growth suppression (Figure 2G), consistent with their roles in transcriptional co-activation of RA-responsive genes.

Aim 2: Determine how cancer-causing mutations in BRCA1 alter their function at its target genes.

We have started to investigate whether the transcriptional activity of BRCA1 and PALB2 is relevant to cancer. We found that BRCA1 mutant cell line HCC1937 displayed aberrant responsiveness to Tumor Necrosis Factor (TNF)-alpha. HCC1937 cells synthesize a truncated BRCA1 protein that is a product of a disease-producing mutant allele (5382insC) and no wild type protein. We used HCC1937 cells that were reconstituted with either wild type BRCA1 construct or vector alone. We observed a robust enhancement of HCC1937 cells reconstituted with wild type BRCA1 compared to the parental lines expressing an empty vector, consistent

with the role for BRCA1 in TNF-alpha (Figure 3A). To gain further insight into the mechanism by which BRCA1 and PALB2 mediate responsiveness to TNF-alpha we asked whether depletion of BRCA1 or PALB2 decrease the recruitment of total RNAPII, its serine 2 or serine 5 phosphorylated forms. Recruitment of RNAPII and its phosphorylated forms is substantially diminished following BRCA1 or PALB2 depletion in genes that displayed corresponding changes in their transcription (Figure 3B).

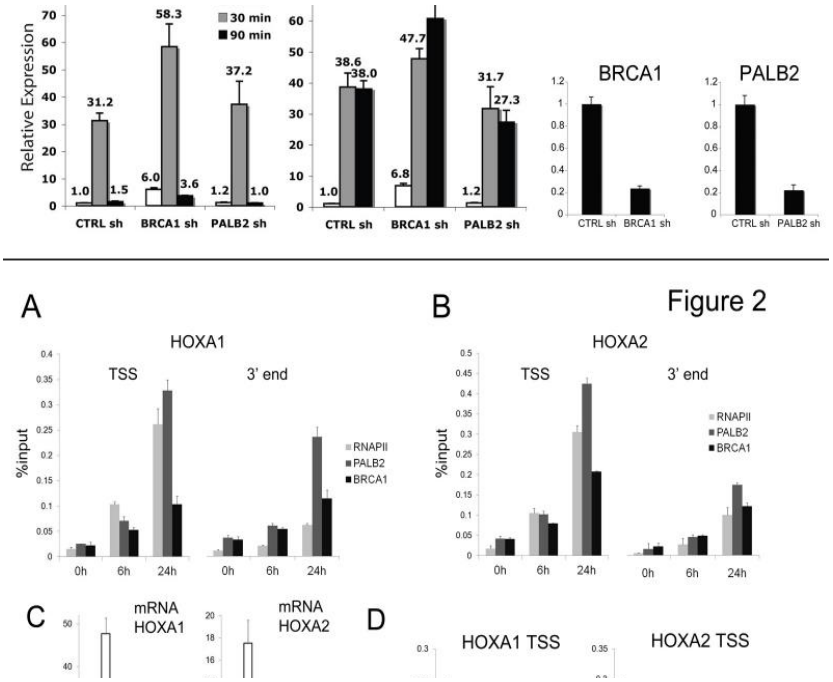

Figure 1.
(**A**) HCT116 cells were transfected with PALB2, BRCA1 and non-targeting (SCR) small hairpin ribonucleic acids (shRNAs), then stimulated with Nutlin-3 for 16 hours to trigger p53 activation. *p53 induced gene 3* (*PIG3)* and *cyclin dependent kinase inhibitor 1A* (*CDKN1A)* expression does not significantly change upon depletion of the breast cancer proteins. Results are the average of 3 independent experiments, data are expressed as fold change over uninduced SCR sh and normalized using *Glucuronidase* (*GUSB)* expression.
(**B**) Analysis of EGF response in HeLa cells transfected with PALB2, BRCA1 and SCR shRNAs. Cells were stimulated with rEGF (100ng/ml) for 30 and 90 minutes. Response of Immediate Early Genes like *Finkel Biskis Jinkins osteosarcoma* (*FOS)* and *Nuclear Receptor 4A1* (*NR4A1)* does not significantly change upon depletion of the breast cancer proteins. Average of 3 independent experiments.

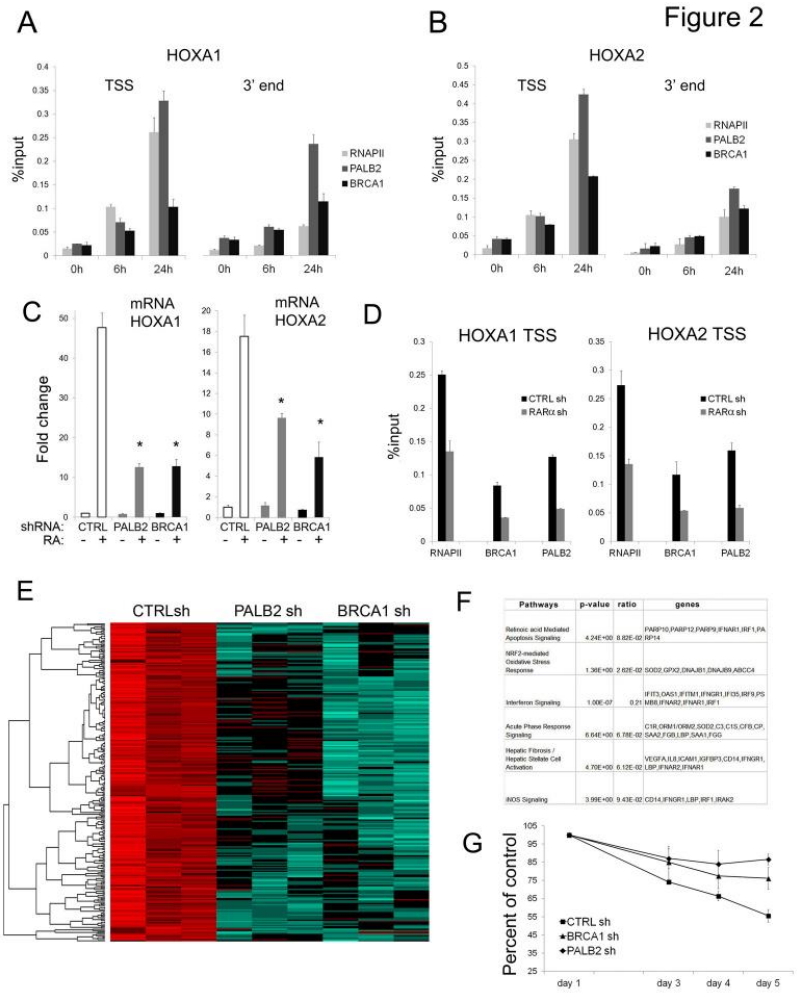

Figure 2.

(**A**) and (**B**) Recruitment of BRCA1, PALB2 and RNAPII at the transcription start site and the 3' end of HOXA1 and HOXA2 genes upon stimulation with 10 uM RA.

(**C**) The expression analysis of HOXA1 and HOXA2 expression was normalized against GUSB expression and is reported as a fold-increase over unstimulated cells (RA -) infected with a non-targeting construct (CTRL).

(**D**) Recruitment of BRCA1 and PALB2 at HOX genes is RARa dependent. Chromatin occupancy of RNAPII, BRCA1 and PALB2 was analyzed upon 6h of RA stimulation in MCF7 cells infected with lentiviral shRNAs against RARa.

(**E**) Global RA transcriptional response is diminished following BRCA1 and PALB2 depletion. The heatmap representation covers 248 microarray probes upregulated by retinoic acid in normal conditions (CTRL shRNAs, expression fold change of t=24h over t=0h, log2(FoldChange)>0.4).

(**F**) The table lists some of the most significant pathways regulated by retinoic acid in MCF-7 cells (Ingenuity Canonical Pathways analysis). (**G**) PALB2 and BRCA1 depletion attenuates RA growth suppression. MCF7 cells stably transfected with shRNAs against BRCA1, PALB2 and CTRL were plated at subconfluent density and treated with 10 uM RA for 5 days.

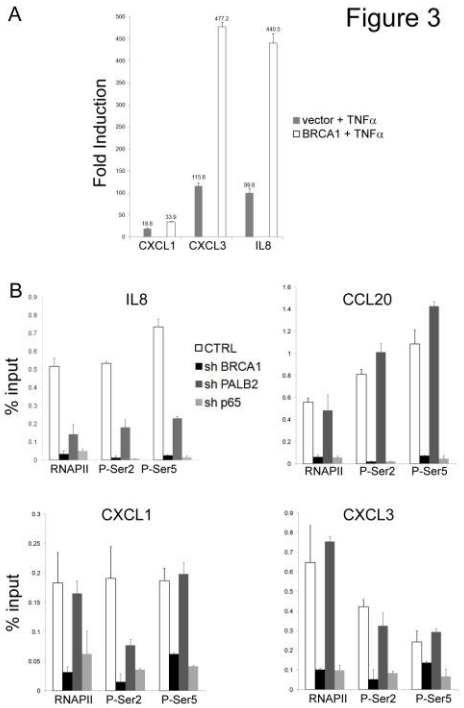

Figure 3**.** *Requirement of BRCA1 for TNF-alpha activation.*
(**A**) Response to TNF-alpha was investigated in HCC1937 cells, which carry one defective allele of BRCA1. Cells stably transfected with the empty vector or stably reconstituted with wild type BRCA1 were stimulated with TNF-alpha for 1h. Fold induction relative to t=0h for each cell line was calculated. Data are normalized to GUSB expression.
(**B**) Analysis of RNAPII and its phosphorylation status in MCF7 cells depleted of BRCA1, PALB2 or p65. qChIP was performed after TNF-alpha stimulation and reveals a substantial impairment of RNAPII recruitment after PALB2 and BRCA1 depletion. BRCA1 also impairs chemokine ligand 1 (CXCL1), chemokine ligand 3 (CXCL3) and chemokine ligand 20 (CXCL20) activation (Figure 2D), which reflects in a severe reduction of RNAPII recruitment.

Research Project 4: Project Title and Purpose

Analysis of Markers of Progression and Therapy Resistance in Melanoma – Melanoma is an aggressive disease for which there is a universally poor prognosis. We have discovered that a dynamic transition of melanoma cells to a mesenchymal phenotype results in a highly invasive and therapy-resistant subpopulation of cells, marked by expression of the protein Wnt5A. This may hold significant implications for novel therapies currently being used to treat melanoma patients, specifically, BRAF inhibitors that are meeting with great success in the clinic, but to which, unfortunately, patients quickly develop resistance. We will test whether inhibiting the Wnt5A signaling pathway can overcome this observed resistance, and elucidate the mechanisms by which Wnt5A contributes to therapy resistance.

Duration of Project

1/1/2013 – 6/30/2014

Project Overview

Melanomas are characterized by a high degree of heterogeneity, invasiveness, and resistance to therapy. Mechanistically, we have shown that the Wnt5a pathway is a critical regulator of mesenchymy in melanoma. We have shown that Wnt5a binds to the receptor tyrosine kinase ROR2, antagonizes canonical Wnt signaling, ultimately conferring a mesenchymal phenotype to melanoma cells. We have recently discovered that this may hold significant implications for novel therapies currently being used to treat melanoma patients. The long-term goal of this research is to define the role of the Wnt5A pathway in therapy resistance.

The BRAF gene is mutated in 50% of melanoma patients, and patients treated with BRAF inhibitors (e.g., PLX4720) demonstrate robust clinical responses, at least for a time. Recently, a requirement for β-catenin and the canonical Wnt pathway for the robust response to BRAF inhibitors has been discovered. These data suggest that the Wnt5A pathway, which inhibits canonical Wnt signaling, might render tumor cells resistant to BRAF inhibitors. To address this we have the following specific aims:

Specific Aim 1. Investigate the role of Wnt5A signaling in resistance to BRAF inhibitors. Using genetic and pharmacologic approaches we will manipulate Wnt5a and determine the response to BRAF inhibitors *in vitro*. We have shown that inhibiting ROR2 *in vitro* and *in vivo* will dramatically increase the effects of BRAF inhibitors. We will ask in this aim, whether resistance can continue to occur in the absence of Wnt5A/ROR2, and if so what mechanisms arise to mediate that resistance.

Specific Aim 2. Investigate whether Wnt5A induces MAPK signaling via CAMKII. Our preliminary data indicate CAMKII signaling may play a role in Wnt5A mediated resistance to Vemurafenib. We hypothesize that Wnt5A also contributes to increased or at least sustained MAPK signaling, in the presence of BRAF inhibitors, via CAMKII activation. We will ask if MAPK signaling is sustained in resistant cells, and if so if CAMKII is an essential intermediate. We will examine the potential of CAMKII inhibitors as adjuvant therapy to BRAF inhibition.

Principal Investigator

Ashani T Weeraratna, PhD
Assistant Professor
The Wistar Institute
3601 Spruce St,
Philadelphia PA 19104

Other Participating Researchers

Michael P. O'Connell, PhD; Marie R. Webster, PhD; Katie Marchbank, PhD – employed by The Wistar Institute

Expected Research Outcomes and Benefits

Current standard of care for melanoma patients includes the use of inhibitors to the mutant form of BRAF, in patients carrying the BRAF V600E mutation. These drugs have met with initial success, but tumors recur, on average, within 7 months of treatment. The need for improving the efficacy and duration of BRAF inhibitors is critical. We have previously shown that Wnt5A is a key mediator of a switch to a mesenchymal, highly invasive state in melanoma. We have also shown that the novel orphan tyrosine kinase receptor, ROR2, is required for the transduction of non-canonical Wnt signals in melanoma. It is known that canonical Wnt signaling, via β–catenin, plays a key role in the genesis of melanoma, but its role in melanoma metastasis is unclear, with most data pointing to a loss of β–catenin activity in metastatic melanoma. This is consistent with the finding that in some cell systems, Wnt5A can inhibit β–catenin activity, by increasing its degradation. Recently, it has been shown that β–catenin can sensitize melanoma cells to BRAF inhibitors. If Wnt5A can inhibit β–catenin then it follows that Wnt5A positive melanoma cells would be more resistant to BRAF inhibitor therapy.

By understanding how Wnt5A modulates the efficacy of BRAF inhibitors, we will be able to design therapies to sensitize cells to BRAF inhibitor therapies. We will also be able to identify patients who may respond well, vs. those who may not. Successful completion of this aim could have far –reaching implications for current advances in melanoma therapy.

Summary of Research Completed

Overall Progress

In the last year, we have focused more on the understanding of how Wnt5A is mediating resistance in melanoma (Aim1) and have taken a more targeted approach to understanding the role of Wnt5A in mediating therapy resistance. We have also expanded our studies for Aim 2. To sum up the accomplishments during this reporting period, we have:

- Infected cells with the lentiviral vectors required for the ras activating factor B (BRAF) experiments (Aim 1).
- Demonstrated that beta-catenin predicts for sensitivity to BRAF inhibitors (Aim 1).
- Demonstrated that Wnt5A drives a p21 mediated stress response to BRAF inhibitors, which can be ameliorated by CAMKII inhibition (Aim 1 and 2).

This work is currently being assembled for publication. The clinical data constitutes one half of a manuscript from our laboratory that was published in the journal *Cancer Discovery*. The beta-catenin and sensitivity studies are also being compiled for *Cancer Discovery*. The Wnt5A-mediated resistance of melanoma cells via p21 is currently under review at our flagship melanoma journal, *Pigment Cell and Melanoma Research*.

Detailed Progress:

1. β -catenin predicts for sensitivity to BRAF inhibitors.

We find that β-catenin low cell lines demonstrate a sensitivity to PLX4720 with an IC50 of around 100-300nM, whereas β- catenin high cells have much higher IC50s ranging from 2 μm to well over 10 μm. Transfecting V600E into b-catenin high cell lines results in cell death (Figure 1). We demonstrate here that in a panel of BRAF inhibitor-sensitive and resistant cell lines (Figure 2A), β- catenin expression is elevated in sensitive cell lines. Further, in a panel of patients, those with good response to BRAF inhibitors (Vemurafenib) had higher levels of β-catenin (Figure 2B,C). Our patient data indicate that the vast majority of β -catenin positivity we see is cytoplasmic, and the reasons for the differences observed in relation to altered cellular localization remain unclear.

2. Wnt5A drives an adaptive stress response via p21.

P21 has been shown to drive senescence, so we tested the ability of targeted therapy to increase p21 in Wnt5A high cells. Wnt5A high cells endogenously express more p21 than Wnt5A low cells (Figure 3A), and appear to be more senescent (Figure 3B). Treatment of Wnt5A low cells with recombinant Wnt5A increases p21 (Figure 3C) and treatment of Wnt5A high cells with siRNA against Wnt5A decreases p21 (Figure 3D). Since protein kinase C (PKC) has been shown to activate p21, and Wnt5A works though the activation of PKC, we asked whether inhibiting PKC could inhibit p21 expression. Cells were pretreated with the PKC inhibitor GO6983, and then exposed to Wnt5A. In the presence of the PKC inhibitor, Wnt5A could not increase p21 expression (Figure 3E). Increases in expression of Wnt5A and p21 are observed after 5 days of treatment with 1 μM PLX4720 in Wnt5A high cells (Figure 3F), but not in Wnt5A low cells (Figure 3G).

Our studies have indicated that samples from patients with a poor clinical response to Vemurafenib (less than 30% response by RECIST), or samples from tumors from patients who relapsed after an initial response expressed high levels of Wnt5A. To determine whether p21 was highly expressed in relapsed samples or samples with a low response rate, we stained 9 samples from patients who exhibited a RECIST response of less than 30%, or which were samples of recurrent, relapsed tumors. Of these 7 exhibited high levels of p21 staining. Of four samples with a strong response to Vemurafenib (greater than 30% response), 2 were negative for p21, 1 had moderate positivity, and one had weak positivity for p21. Even in this small sample set, this was significant to $p=0.03$ using a two-tailed t-test. Shown as a comparison are samples with >30% response rate, which show little p21 expression, as compared to ones with a <30% response rate (Figure 3H).

3. CAMKII sensitizes melanoma cells to BRAF inhibitors.

Next, we examined resistant subclones of melanoma cells that had been exposed to PLX4720. These subclones demonstrate the ability to sustain mitogen activated protein kinase (MAPK) signaling even when treated with PLX4720 (Figure 4A). Since Wnt5A can signal to sustain MAPK activity, we examined the resistant subclones for Wnt5A expression. We find that BRAF resistant subclones increase their Wnt5A and p21 expression (Figure 4B). These same clones increased their PO4-CAMKII expression (Figure 4C) consistent with our hypothesis that Wnt5A signals to sustain MAPK signaling via CAMKII. Treating Wnt5A high, resistant cells with an inhibitor of CAMKII (KN93) decreases Wnt5A and p21 (Figure 4D). We then treated cells with KN93, and asked whether inhibiting these signals increased sensitivity to PLX4720. We find that

KN93 does not affect cell viability on its own (Figure 4E), but pre-treatment with KN93 sensitizes cells to PLX4720, decreasing the IC50 almost ten-fold (Figure 4F). These data indicate that the inhibition of CAMKII may be a worthwhile pursuit for increasing the efficiency of targeted therapy.

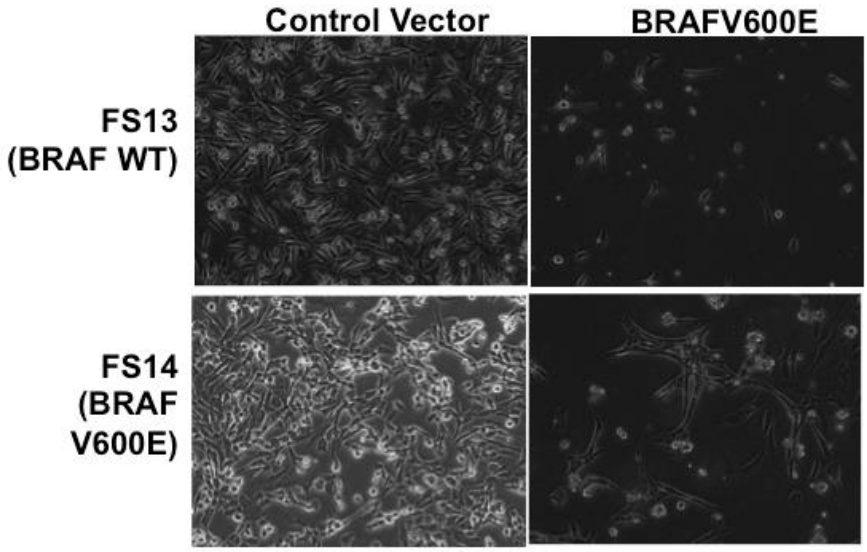

Figure 1. *Transfection of BRAFV600E into melanoma cells results in cell death*. Two melanoma cell lines, one wild type for BRAF (FS13), and one already containing BRAFV600E were infected with either a control lentivirus, or one with the BRAFV600E gene. In both cell lines, V600E introduction was detrimental to the health of the cells.

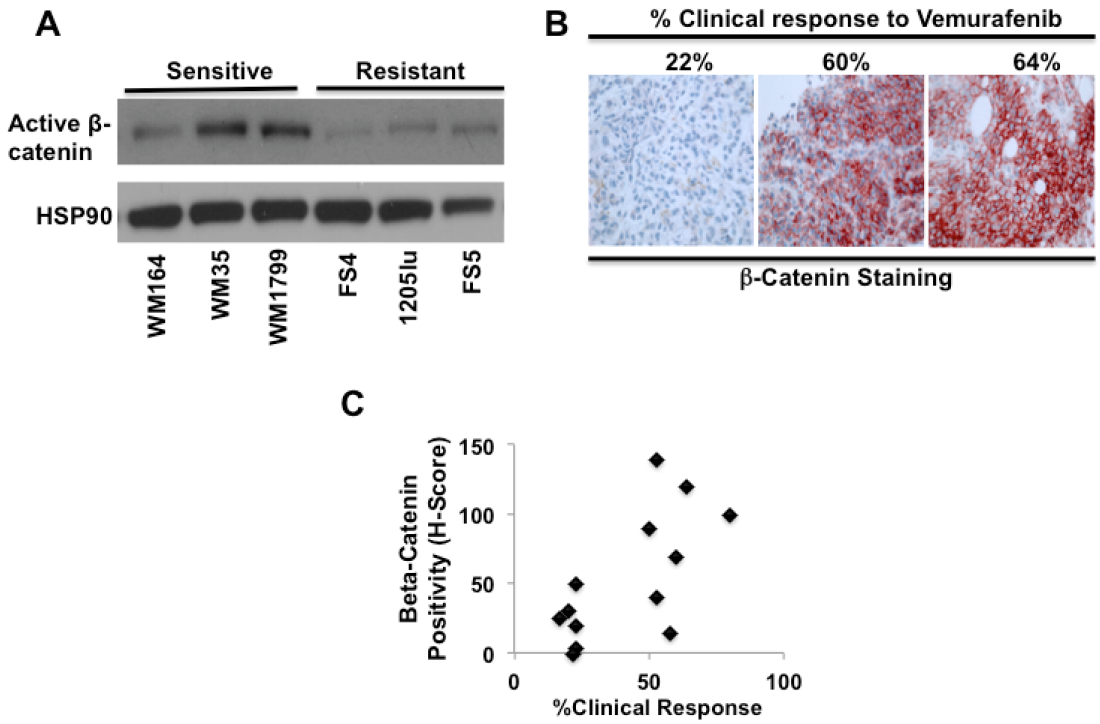

Figure 2. *Beta-catenin predicts for sensitivity to BRAF inhibitors*. In a panel of BRAF inhibitor-sensitive and resistant cell lines, β- catenin expression is elevated in sensitive cell lines (A). Further, in a panel of patients, those with good response to BRAF inhibitors (Vemurafenib) had higher levels of β-catenin (B,C).

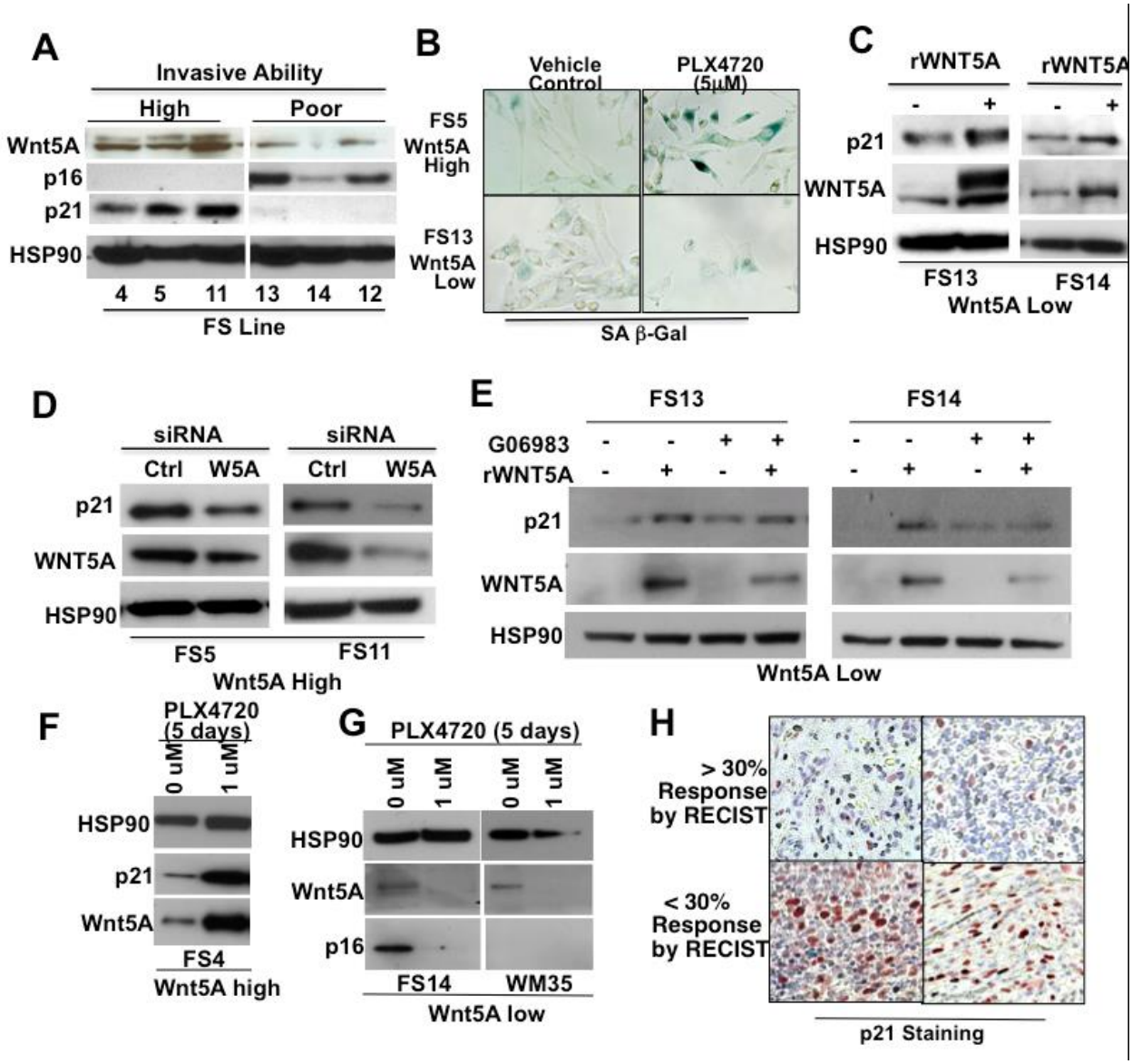

Figure 3. *Wnt5A regulates p21 expression in melanoma*. (A) Western analysis of cell cycle regulators, p16 and p21 in Wnt5A-high and Wnt5A-low cells. (B) Wnt5A-high cells were positive for SA-b-galactosidase whereas Wnt5A-low cells were largely dead at 5 days post-treatment with PLX4720. (C) Treatment of Wnt5A-low cells with rWnt5A increases p21 expression and (D) knockdown of Wnt5A in Wnt5A-high cells decreases p21 expression by Western analysis. (E) Inhibition of PKC using GO6983 inhibits the ability of rWnt5A to increase p21. p21 expression remains high in (F). Wnt5A-high melanoma cells following 5 days of treatment with PLX4720, but not in (G) Wnt5A-low melanoma cells. Patient samples with > 30% and <30% response by RECIST were stained for p21 expression by IHC (H).

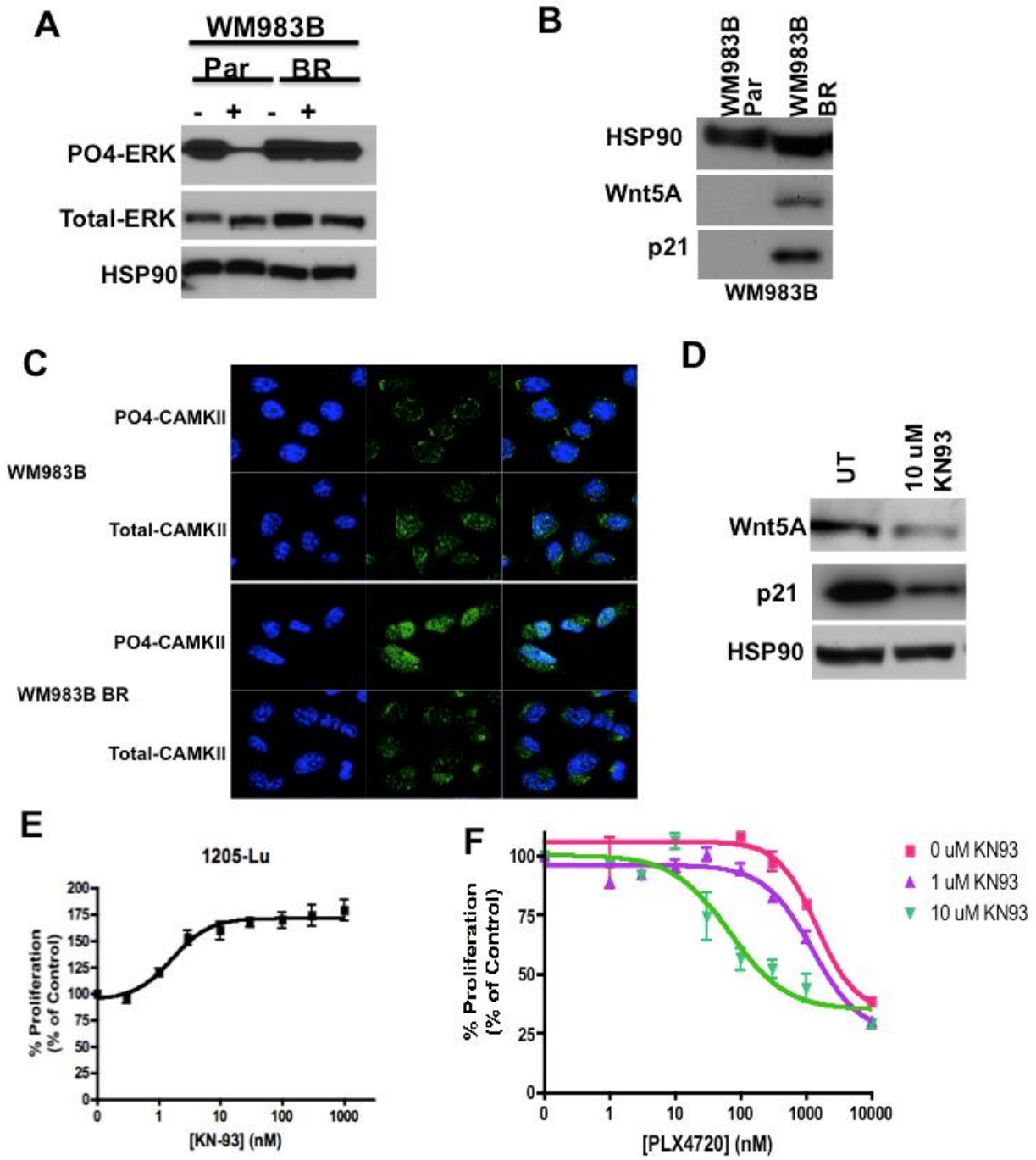

Figure 4. *Inhibition of CAMKII inhibits Wnt5A mediated resistance*. Resistant subclones sustain MAPK activity even in the presence of inhibitor (A). BRAF resistant subclones increase their Wnt5A and p21 expression (B). These same clones increased their PO4-CAMKII expression (C) Treating Wnt5A high, resistant cells with an inhibitor of CAMKII (KN93) decreases Wnt5A and p21 (D). KN93 treatment alone does not inhibit cell viability (E), but pre-treatment with KN93 sensitizes cells to PLX4720 (F).

Research Project 5: Project Title and Purpose

Developing Rational Strategies for Therapeutic Targeting of NRAS-Mutant Melanomas – Mutations in NRAS are found in approximately 25% of melanomas. These tumors are extremely aggressive and are among the most difficult tumors to treat. Unfortunately, there are no effective therapies to treat patients with NRAS mutant melanomas. Targeting NRAS itself has thus far not been successful; therefore, alternative strategies are necessary. *The goal of this project is to identify key molecules that promote survival of NRAS mutant melanomas.* These essential molecules could be potential targets for the treatment of NRAS mutant melanomas. We postulate that blocking critical molecules that are essential for survival of NRAS mutant tumors can kill these neoplasms.

Duration of Project

1/1/2013 – 6/30/2014

Project Overview

Melanoma, the most lethal form of skin cancer, is caused by genetic mutations in multiple genes, frequently in genes coding for two proteins called BRAF and NRAS. BRAF and NRAS control critical cellular functions through a series of biochemical reactions known as signaling pathways. Despite recent advances treating melanoma, there are no effective therapies for about ~25% of melanomas carrying NRAS mutations. Hence, effective treatments for NRAS mutant melanomas are urgently needed.

An essential requirement to develop effective treatments for NRAS mutant melanomas is to understand the chain of molecular events activated by NRAS. Unfortunately, very little is known about the molecular pathways that are activated by mutant NRAS, and this gap in knowledge hampers the development of effective therapies. Therefore, it is critical to identify the signaling molecules that are activated by NRAS that are essential for tumor survival. *This project aims to identify critical signaling molecules activated by NRAS that are essential for survival of NRAS mutant melanomas.* Two specific aims are proposed:

<u>Aim 1. Define the molecular consequences of silencing oncogenic NRAS in melanoma</u>. The goals of this aim are: a) to identify human melanoma cells that are dependent of NRAS signaling for proliferation and survival, and b) to determine the biochemical effects of silencing NRAS in melanomas harboring mutations in this oncogene.

<u>Aim 2. Identify genes or pathways that when targeted can potently kill NRAS mutant melanomas</u>. We will evaluate the effect of treating NRAS mutant melanoma cells with drugs that block RAS effector molecules. For these studies we will use cells that have been isolated from melanoma patients and grown in the laboratory.

We expect that our studies will help us identify new drug targets that will help develop effective treatments for melanoma patients.

Principal Investigator

Jessie Villanueva, PhD
Assistant Professor
The Wistar Institute
3610 Spruce Street, Room 307
Philadelphia, PA 19104

Other Participating Researchers

Patricia Reyes-Uribe, BS; Hsin-Yi Chen, PhD; Minu Samanta – employed by The Wistar Institute

Expected Research Outcomes and Benefits

Melanoma is the most fatal form of skin cancer. The incidence of melanoma has been progressively increasing with over 70,000 melanoma cases diagnosed and close to 9000 deaths every year in the US. Despite recent advances in treating this cancer, the survival rate is less than 5% and the median survival is 6-12 months.

Although NRAS is the second most frequently mutated oncogene in melanoma, there are no therapeutic options currently available for NRAS-mutant melanomas and very little is known about the effector pathways that mediate survival of these tumors. Furthermore, mutations in NRAS correlate with poor clinical outcome and shorter survival. Consequently, effective therapies for NRAS mutant melanomas, which comprise 15-30% of tumors, are urgently needed. Our proposed studies will fill a significant knowledge gap in the field and will have significant clinical and public health implications. Our studies are important because the identification of critical RAS effectors will provide therapeutic targets to control NRAS mutant tumors.

RAS mutations were identified more than three decades ago and are frequently present in a large number of human cancers. Notably, RAS mutant tumors are among the most difficult cancers to treat. Hence, rational treatment options are sorely needed. We anticipate that the proposed studies will have a major impact on the treatment of melanoma and other RAS-driven cancers. The data generated by our studies will be crucial for understanding RAS signaling in melanoma and improving the treatment of this aggressive disease.

Summary of Research Completed

During this reporting period we have made substantial progress in Aim 1A of this project and have initiated Aim 2 as detailed below:

<u>Aim 1. Define the molecular consequences of silencing oncogenic nueroblastoma RAS viral oncogene homolog (NRAS) in melanoma.</u>

The goals of this aim are:

A. To identify human melanoma cells that are dependent of NRAS signaling for proliferation and survival. In the previous reporting period we included the initial results of this sub aim. During this reporting period we have extended our studies and further confirmed our preliminary findings using complementary strategies.

Silencing NRAS inhibits proliferation of melanoma cells

To evaluate the biological consequences of silencing NRAS in melanoma, we selected a panel of NRAS mutant cells. All cell lines have been sequenced to determine the NRAS mutation status. We generated four melanoma cell lines expressing NRAS small hairpin ribonucleic acid (shRNA). Depletion of NRAS in these cell lines was confirmed by immunoblotting (Figure 1); NRAS levels were decreased by >75% after lentiviral infection in all cell lines.

To determine the effect of NRAS silencing on proliferation, we assessed the expression of the proliferative marker Ki67 by immunofluorescence in NRAS mutant melanoma cells expressing an shRNA non-targeting control or NRAS-shRNA. Approximately $2x10^4$ cells expressing shRNA control or shNRAS were seeded onto cover slips, allowed to attach and spread and grow for 24h. The next day the media was removed and the cells fixed with 4% paraformaldehyde. Cells were then permeabilized with 0.2% w/v Triton X-100 for 5 minutes and then blocked with 1% Bovine serum albumin (BSA) in phosphate buffer saline (PBS) for 30 minutes at room temperature followed by incubation with anti-Ki-67 antibody for 1h at 37°C. After washing, secondary antibody was added to the coverslips and incubated for 1h at 37°C, followed by 3 washes with PBS and finally transferred to a slide by placing them over a drop of ProLong Gold with DAPI (4',6-diamidino-2-phenylindole) and sealed. The slides were examined by fluorescence microscopy using a Nikon TE2000 -U microscope with a 20x Nikon Plan Fluor, NA .30 objective and photographed using a Digital camera (Q imaging EX I). We further recorded, processed, and quantified the number of Ki67 positive cells using image analysis software Image Pro Plus 7.0 (Media Cybernetics); image Dimensions were 1360 x 1036 px. To this end, we used two channels:

- Channel 1, Dapi with Exposure: 533ms, Binning: 1 x 1, Gain: 4.000000
- Channel 2, Ki67 with exposure: 500 ms, Binning: 1 x 1, Gain: 4.000000

The total number of cells was determined and quantitated using the channel 1 (Dapi), whereas Ki67 positive cells were determined and quantitated using channel 2. Both images were merged using the same software (Figure 2). We observed that NRAS mutant melanomas transduced with a control shRNA were positive for Ki67, whereas depletion of NRAS substantially decreased the number of Ki67 positive cells (Figure 2), indicating that loss of NRAS inhibits proliferation of NRAS mutant melanomas. Similar results were obtained in all cell lines tested (data not shown). To further validate the effect of silencing NRAS on melanoma proliferation, we evaluated growth rate of NRAS mutant melanomas transduced with a non-targeting shRNA or NRAS shRNA. For this experiment $5X10^4$ cells were seeded onto 12-well plates. Cells were fixed with methanol every 24 hours for 5 days. At the end of the time course, the cells were stained with crystal violet followed by elution of the dye with 0.1 M trisodium citrate in 50% ethanol for 10 min. Optical density at 595 nM was monitored on a microtiter plate reader in duplicates. The crystal violet assay further confirmed that depletion of NRAS decreases cell proliferation (Figure 3).

B. Determine the biochemical effects of silencing NRAS in melanomas harboring mutations in this oncogene.

Total protein lysates from NRAS mutant melanoma cells expressing a non-targeting shRNA or NRAS shRNA were analyzed by immunoblotting to determine the effect of NRAS depletion on levels or activity of potential NRAS effectors (Figure 4). We found that NRAS depletion inhibited (mitogen activated protein kinase) MAPK signaling evidenced by decreased phosphorylation of MEK (MAP and ERK kinase) and ERK (extracellular regulated kinase) in all cell lines tested. However, NRAS depletion did not inhibit phosphorylation of AKT (or Protein kinase B; PKB) at Ser473 or Thr308. Moreover, NRAS depletion appears to increase phospho-AKT levels. The levels of NRAS, phospho-MEK and phospho-ERK were quantified using the LiCor Oddysey system (Fig. 5)

<u>Aim 2. Identify genes or pathways that when targeted can potently kill NRAS mutant melanomas.</u>

During this reporting period we have initiated studies aimed at blocking RAS (Rous sarcoma virus) effector molecules and evaluating the biological consequences of pharmacological inhibitors.

Since our initial studies indicated that NRAS depletion decreased MAPK signaling as described above, we wished to investigate the effect of inhibiting the MAPK pathway using small molecule inhibitors. To this end we treated NRAS mutant melanoma cells with the allosteric MEK inhibitor Trametinib at different concentrations for 24, 48, or 72 hours. Trametinib effectively inhibited the MAPK pathway as evidenced by decreased phosphorylation of MEK, ERK, and RSK (ribosomal S6 kinase). MAPK inhibition was coupled to inhibition of Cyclin D1 expression and phosphorylation of retinoblastoma (Rb) indicative of inhibition of cell cycle progression. MAPK inhibition at 48 and 72h also led to accumulation of cleaved lamin A, a marker of apoptosis. To further evaluate the effect of MAPK inhibition on proliferation we seeded $5X10^4$ cells onto 12-well plates. Cells were fixed with methanol every 24 hours for 10 days. At the end of the time course, the cells were stained with crystal violet as described above (Aim 1A). The relative number of cells in each plate was assessed by reading absorbance at 595 nM. Treatment of NRAS mutant melanoma cells with trametinib decreased growth compared with cells treated with vehicle control (Figure 6).

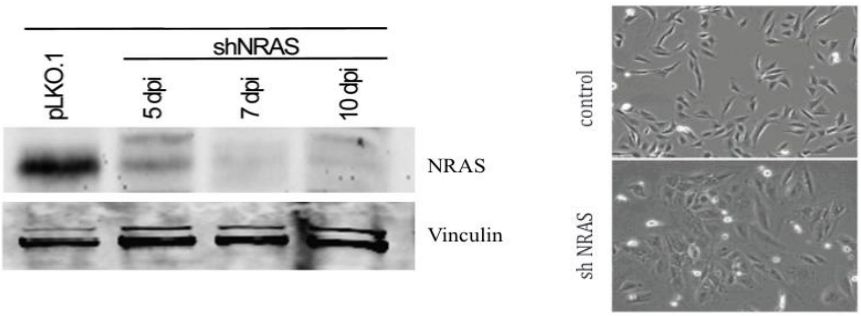

Figure 1. Efficient lentiviral mediated knock down of NRAS in melanoma cells. A representative cell line is shown to depict efficient knock of NRAS after 5, 7 or 10 days (dpi) post transduction. Similar results in terms of silencing efficiency and kinetics were observed in most NRAS mutant melanoma cell lines. Melanoma cells transduced with NRAS shRNA displayed an altered morphology (right panels).

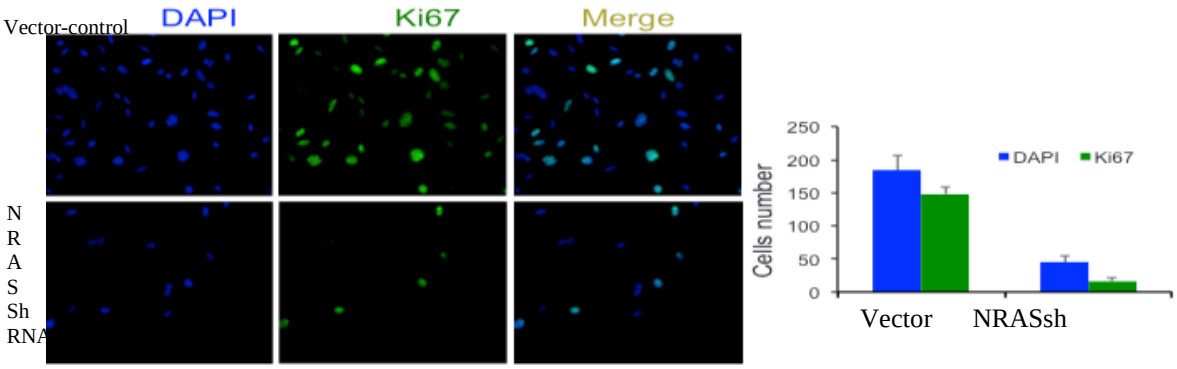

Figure 2. Depletion of NRAS decreases cell proliferation. NRAS mutant melanoma cells were transduced with a non-targeting shRNA vector control or NRAS shRNA. Transduced cells were stained with the proliferative marker Ki67 (green) and DAPI (blue) to visualize the nucleus. More than 80% of the cells transduced with a vector control were Ki67 positive. Depletion of NRAS caused a decrease in the total number of cells; furthermore, NRAS depletion caused a substantial decrease in proliferation evidenced by the loss of Ki67 positive cells.

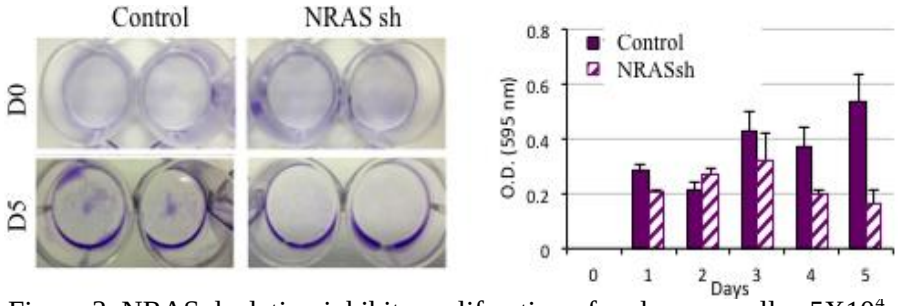

Figure 3. NRAS depletion inhibits proliferation of melanoma cells. $5X10^4$ melanoma cells transduced with either a non-targeting shRNA or a lentiviral vector carrying a NRAS shRNA construct were seeded onto 12-well culture plates in duplicate, collected every 24 hours for 5 days. Cells were fixed with methanol and stained with crystal violet. Representative images are shown for D0 and D5 (left panels). Relative number of cells was assessed by measuring absorbance at 595 nm. Absorbance was plotted against time and results of a representative cell line are shown in the graph on the right panel.

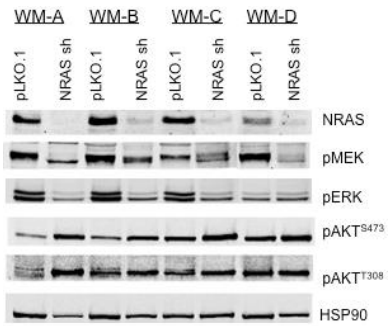

Figure 4. NRAS silencing inhibits MAPK signaling. NRAS mutant melanoma cells were transduced with a non-targeting shRNA or NRAS shRNA. Total cell lysates were analyzed by immunoblotting with the indicated antibodies.

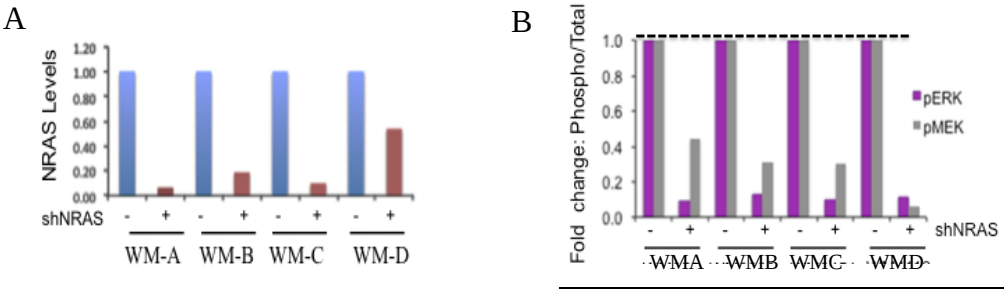

Figure 5. NRAS depletion decreases pMEK and pERK levels. (A) Levels of NRAS were quantified using the LiCor Oddysey system. Relative NRAS levels following transduction with NRAS shRNA were determined by normalizing signal intensity relative to signal intensity in lysates from isogenic cells transduced with a non-targeting shRNA. (B) Relative phosphorylation of MEK and ERK was assessed as in A. Fold change in phosphorylation was calculated by normalizing the intensity of phospho-protein signal relative to total protein levels in each condition for each isogenic pair of cells.

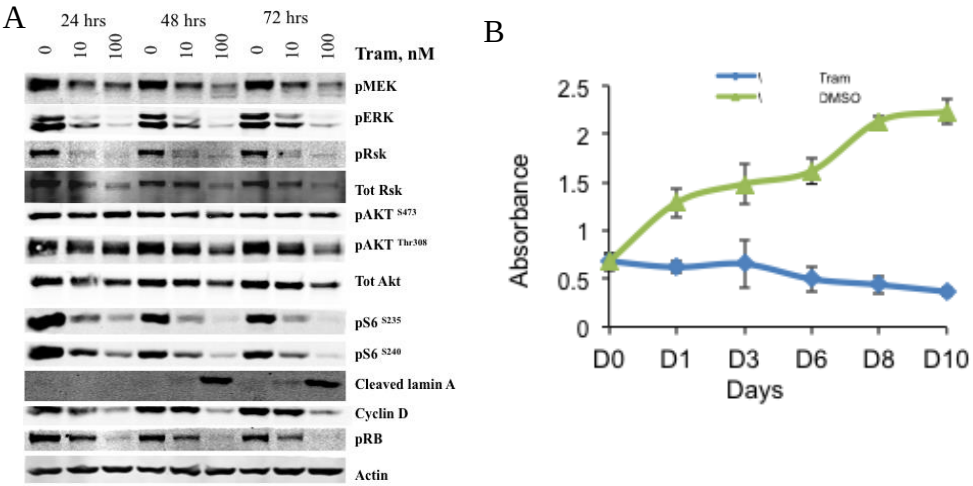

Figure 6. MEK inhibition inhibits proliferation of some NRAS mutant melanoma cells. (A) NRAS mutant melanoma cells were treated with different concentrations (0, 100, or 1000 nM) of the allosteric MEK Inhibitor Trametinib. Total cell lysates were analyzed by immunoblotting for the indicated proteins. (B) NRAS mutant melanomas were treated with 100 nM of Trametinib for different times (0-10 days). Proliferation of NRAS mutant melanomas.